KSOE

Prediction of Wave Transmission Characteristics of Low Crested Structures Using Artificial Neural Network

Taeyoon Kim[1], Woo-Dong Lee[2], Yongju Kwon[3],
Jongyeong Kim[3], Byeonggug Kang[3] and Soonchul Kwon[4]

[1]Research Professor, Department of Ocean Civil Engineering, Gyeongsang National University, Tongyeong, Korea
[2]Professor, Department of Ocean Civil Engineering, Gyeongsang National University, Tongyeong, Korea
[3]Student, Department of Civil Engineering, Pusan National University, Busan, Korea
[4]Professor, Department of Civil Engineering, Pusan National University, Busan, Korea

ABSTRACT: Recently around the world, coastal erosion is paying attention as a social issue. Various constructions using low-crested and submerged structures are being performed to deal with the problems. In addition, a prediction study was researched using machine learning techniques to determine the wave attenuation characteristics of low crested structure to develop prediction matrix for wave attenuation coefficient prediction matrix consisting of weights and biases for ease access of engineers. In this study, a deep neural network model was constructed to predict the wave height transmission rate of low crested structures using Tensor flow, an open source platform. The neural network model shows a reliable prediction performance and is expected to be applied to a wide range of practical application in the field of coastal engineering. As a result of predicting the wave height transmission coefficient of the low crested structure depends on various input variable combinations, the combination of 5 condition showed relatively high accuracy with a small number of input variables defined as 0.961. In terms of the time cost of the model, it is considered that the method using the combination 5 conditions can be a good alternative. As a result of predicting the wave transmission rate of the trained deep neural network model, MSE was 1.3×10^{-3}, I was 0.995, SI was 0.078, and I was 0.979, which have very good prediction accuracy. It is judged that the proposed model can be used as a design tool by engineers and scientists to predict the wave transmission coefficient behind the low crested structure.

1. Introduction

As climate change causes sea levels to rise, which increases the external forces of high waves, shoreline deformation with coastal erosion and scour has received significant attention, becoming an important social issue in many countries. In particular, morphological changes in seabed due to such coastal erosion and sedimentation can cause changes in the coastal environment and ecosystems. Various deformation methods have been proposed to recover coastal erosion issues, but commercially utilized gravity-type structures such as breakwaters and headlands change the sea environment, resulting in bad seawater circulation and poor water quality. Low-crested and submerged structures (LCS), such as detached breakwater and artificial reefs, diminish the wave height with reduced wave energy behind a structure due to the change in the freeboard at the still water surface, which protects the inland sea environment. The construction

of LCS is performed under specific conditions to produce the desired wave transmission coefficient; thus, the calculation or prediction of the transmission coefficient of the structure should be carried out as an important factor in designing the structure. To determine the wave transmission coefficient of LCS, various studies have proposed formulas for calculating the wave transmission rate, but the wave transmission coefficients are estimated through a regression analysis of mathematical experimental data, showing a limited analysis of the natural phenomena (Koosheh et al., 2020; Formentin et al., 2017). Recently, a machine learning model has been used to estimate and predict statistical structures from input and output data. This machine learning model can readily explain the regression analysis of nonlinear relationships (Hashemi et al., 2010; Rigos et al., 2016). Machine-learning-based prediction models employ deep learning algorithms of neural networks, which have been continuously applied in the field of coastal engineering in recent years, especially for solving problems

related to modeling behavior around coastal structures (Shamshirband et al., 2020; Kim et al., 2005; Formentin et al., 2017; Panizzo and Briganti, 2007).

Herein, we introduced a prediction trend of the wave attenuation characteristics of LCS to propose an explicit method composed of weights and biases using artificial neural network. To estimate dominant factors for the wave transmission rate of LCS, we applied machine learning models to predict the wave height transmission rate of LCS dependent on 7 types of dimentionless characters with sensitivity analysis. In addition, we proposed an optimized machine learning model suitable for the determination of wave transmission coefficient and performs an overall analysis of the model with various combination. Finally, we carried out the evaluation of the applicability of the machine learning model through the analysis of the accuracy associated with the formulas for calculating the wave height transmission rate of the existing LCS. We found that the estimated wave attenuation characteristics calculated with the presented weight and bias matrix shows better accurate reliability compared with those obtained from the broadly used empirical formula.

2. Background

2.1 Analysis of Transmission Coefficient Empirical Formulas

Among various studies, Takayama et al.(1985) proposed the Eq. (1) to determine the wave transmission coefficient for LCS based on empirical experiment using irregular wave as follows:

$$K_T = -0.92\left(\frac{B}{L_0}\right) + 0.42\left(\frac{R_C}{H_0'}\right) + 3.80\left(\frac{H_0'}{L_0}\right) + 0.51 \tag{1}$$

where B is the crown width, R_C is the crown freeboard, L_0 is deep sea wave length , H_0' is calculated wave height of deep sea. When the relative width of structure increases over a certain value, the value of wave transmission coefficient at $B/L_0 > 0.7$ is defined as a negative value based on the result of Takayama et al.'s(1985) experiment, which was determined using a small with of structure ($B/L_0 < 0.4$) (Lee and Bae, 2020). Thus, it is suitable for an experiment with a short wave period length. In DELOS (Environmental Design of Low Crested Coastal Defence Structures, EVK3-CT-2000-00041) project, more than 2300 two-dimensional experiments were performed to determine the wave transmission coefficient for LCS. Van der Meer et al. (2005) proposed the experimental formula to estimate the wave transmission coefficient using converted dimensionless variables of relative freeboard (R_C/H_i), relative crest width (B/H_i), surf similarity parameter ($\xi = \tan\alpha / \sqrt{H_i/L_0}$) obtained from DELOS as follows:

$$K_T = -0.3\left(\frac{R_C}{H_i}\right) + 0.75(1 - e^{-0.5\xi}), \xi < 3 \tag{2}$$

$$K_T = -0.3\left(\frac{R_C}{H_i}\right) + 0.75\left(\frac{B}{H_i}\right)^{-0.31}(1 - e^{-0.5\xi}), \xi > 3 \tag{3}$$

where $\tan\alpha$ is breakwater slope and effective range of wave transmission coefficient is determined between 0.075 and 0.8.

Goda and Ahrens (2009) proposed the formula of wave transmission coefficient for LCS as follows.

$$K_T = \max\left\{0, \left(1 - \exp\left[a\left(\frac{R_C}{H_i} - F_0\right)\right]\right)\right\} \tag{4}$$

$$a = 0.248\exp\left[-0.384\ln\left(\frac{B_{eff}}{L_0}\right)\right] \tag{5}$$

$$F_0 = \begin{cases} 1.0 & : D_{eff} = 0 \\ \max\{0.5, \min(1.0, H_i/D_{eff})\} & : D_{eff} > 0 \end{cases} \tag{6}$$

where F_0 is dimensionless limit wave run-up height, D_{eff} is the effective diameter of the materials composed of LCS.

$$B_{eff} = \begin{cases} B_{swl} & emerged\,crest \\ \frac{9}{10}B + \frac{1}{10}B_0 & zero\,freeboard \\ \frac{8}{10}B + \frac{2}{10}B_0 & aubmerged\,crest \end{cases} \tag{7}$$

Herein, B_{eff} is effective crest width at still water level, B_{swl} is the width of structure at still water level, B is the crest width of structure, B_0 is the width at the bottom of structure.

Calabrese et al. (2003) used the large-scale experimental data to determine the wave transmission coefficient.

$$K_T = a\frac{R_C}{B} + b \tag{8}$$

$$b = \alpha \times exp\left(-0.0845\frac{B}{H_i}\right) \tag{9}$$

$$\alpha = 1 - 0.562\exp(-0.0507\xi) \tag{10}$$

$$a = \beta \times exp\left(0.2568\frac{B}{H_i}\right) \tag{11}$$

$$\beta = 0.6957 \times \frac{H_i}{h} - 0.7021 \tag{12}$$

2.2 Artificial Neural Network

Artificial neural network (ANN) is modeling systems that provides a data process structure inspired by the neural networks of human brains, which are composed of a web of millions of interconnected neurons. A neuron is a special biological cell that conveys information from one neuron to others. ANN is composed of a large number of simple processing elements interconnected with each other. The system requires the involvement of a labeled direct graph structure where nodes conduct computations. The "directed graph" provides a set of "nodes" (vertices) and a set of "connections" (edges/links/arcs) to connect pairs of nodes. In a neural network, each node performs simple computations, and each connection delivers a signal from one
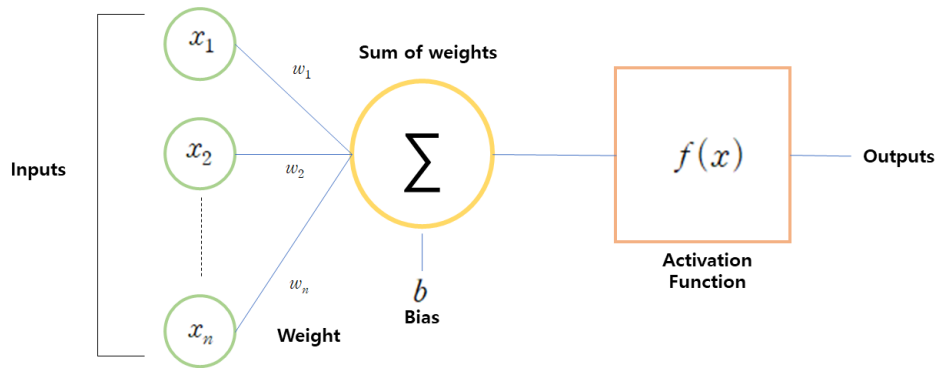
Fig. 1 Neural network diagram of element

node to another, labeled by a number called the "connection strength" or "weight", which implies the extent to which a signal is amplified or diminished by connection, as shown in Fig. 1.

In the ANN data process, the result values are derived by substituting the normalized input variable into the function of Eq. (13) at each node.

$$N_j = \sum_{i=1}^{N_c} w_{ij} x_i + \theta_j \tag{13}$$

where w is weight), θ is Bias, x is input value.

2.2.1 Activation function

The activation function provides the explanation of non-linearity by substituting the estimated input data in each node into a function that creates non-linearity and then outputs the results. Different kinds of functions, such as linear, exponential, sigmoid, tanh, rectified linear unit (ReLU), softmax, scaled exponential linear unit (SeLU), and expoenetial linear unit (elU) are utilized for the activation function. The mean squared error of the various functions where six different activation functions are described to the hidden layer and output layer as shown in Fig. 2.

2.2.2 Gradient decent method

In general, the error back propagation method is used as an optimization algorithm for parameter estimation, which re-updates any parameter to the one with the lowest error. The period in which each parameter is updated once is called the weight adjustment period (epoch). Here, the error backpropagation refers to the process of minimizing the error by re-correcting the weight while going backwards the result of the sum of the errors of each neuron. For the optimization of the loss function, the gradient descent method was developed by re-updating the weights to find the lowest point of the lost value. The existing gradient descent method can accurately derive
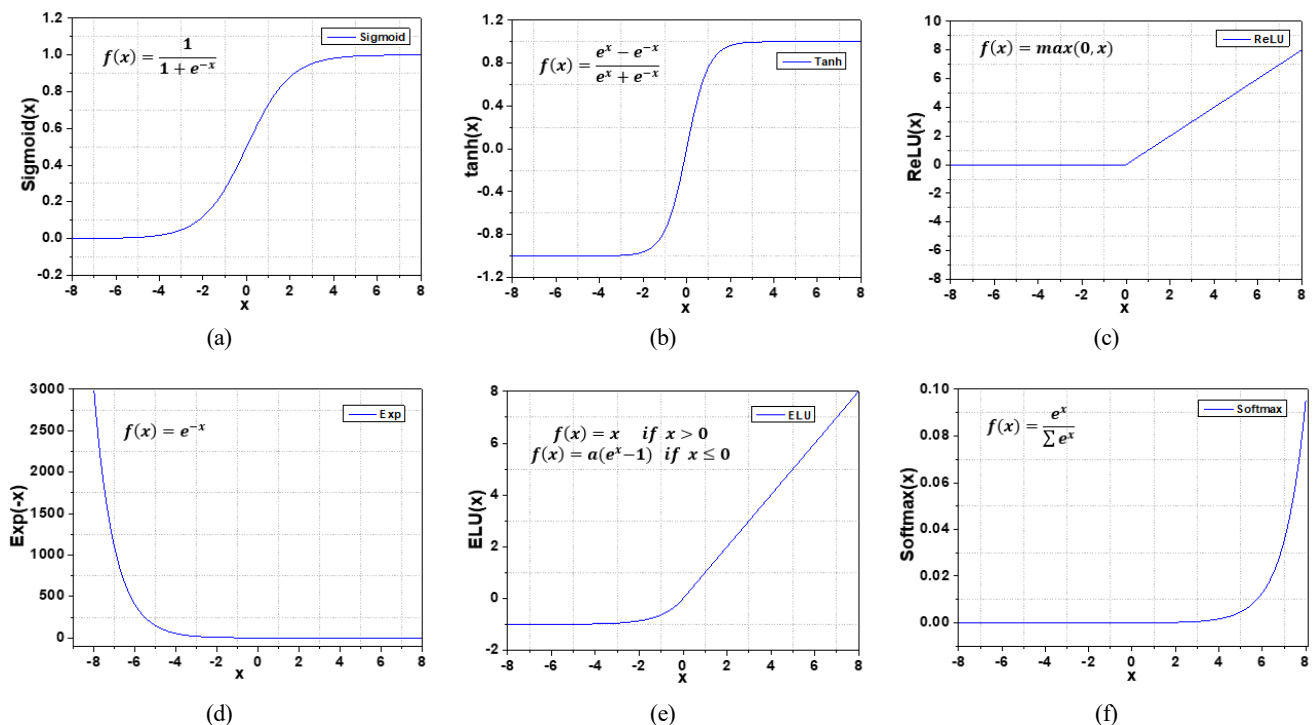

Fig. 2 Type of activation functions: (a) Sigmoid type; (b) Tanh type; (c) ReLU type; (d) Exponential type; (e) eLU type; (f) Softmax type

weights, but it has a disadvantage in that the amount of calculation is very large because it must be differentiated over the entire data instantaneously whenever the weights are changed. That is, the speed may decrease due to the load caused by a large amount of computation, and learning may be stopped before additionally finding the optimal solution. To compensate for this problem, various advanced gradient descent techniques have been developed. Advanced gradient descent techniques include stochastic gradient descent (SGD), momentum, Nesterov accelerated gradient, Adagrad, and root mean square propagation (RMSProp), Adam, etc., and in this study, the optimization process using Adam was performed. Adam is a gradient descent method that combines Momentum and RMSprop techniques, and uses the exponential average of the squares of the slopes of the RMSprop technique. is as follows (Eqs. (14)–(16)).

(1) Stochastic gradient descent (SGD)

The stochastic gradient descent method consists of a set of parameters to be updated through the calculation of the change rate of the loss function (E) and the learning rate (η) shown in Eq. (14).

$$W_{t+1} = W_t - \eta \frac{1}{\sqrt{\hat{h}_t + \epsilon}} \hat{m}_t \tag{14}$$

Here, W is a weight, η is a learning rate, E is an error, and is a method of updating weights according to a constant learning rate (η) using some randomly extracted data.

(2) Adaptive gradient, Adagrad

In the adaptive gradient method, the learning rate is adjusted according to the number of updates of the variable by h_t when the weights are re-updated, and the weights are trained to reach the optimal value. It is a method of learning by decreasing the learning rate for variables that have changed significantly and increasing the learning rate for variables with small changes (Eqs. (15), (16)).

$$W_{t+1} = W_t - \eta \frac{1}{\sqrt{h_t}} \frac{\partial E}{\partial W_t} \tag{15}$$

$$h_t = h_{t-1} + \left(\frac{\partial E}{\partial W_t} \right)^2 \tag{16}$$

Here, for weight update, the learning rate is multiplied by $\frac{1}{\sqrt{h_t}}$, and h_t is the continuous sum of the squares of the slope of the loss function. In addition, in the existing gradient descent method, the addition of the squares of the weight gradients causes the learning rate to decrease gradually for the weights that have a lot of fluctuations in the weight values. However, if Adagrad learns infinitely, at some point h becomes too large and the learning rate becomes 0 and learning is stopped. That is, it works well for the problem of the cost function composed of a simple quadratic equation, but it has a problem that the

learning rate is too reduced and the learning stops completely before reaching the global minimum.

(3) RMSprop

In the complex structure of Adagrad, there is a problem that the learning rate becomes 0 before reaching the global minimum. To compensate for this, the RMSprop technique was developed (Eqs. (17), (18)). This method improved the existing problems by reflecting and accumulating the latest slope information using the Decaying mean.

$$W_{t+1} = W_t - \eta \frac{1}{\sqrt{h_t + \epsilon}} \frac{\partial E}{\partial W_t} \tag{17}$$

$$h_t = \rho h_{t-1} + (1-\rho) \left(\frac{\partial E}{\partial W_t} \right)^2 \tag{18}$$

Here, ρ is added to the h_t parameter, which usually uses a value of 0.9 as the attenuation rate, and functions to reflect the latest gradient information rather than simply accumulating the weight gradient.

(4) AdaDelta (Adaptive delta)

AdaDelta is calculated using the Hessian matrix instead of the learning rate to compensate for the problem of small learning rate in Adagrad, and is calculated as follows Eqs. (19)–(22).

$$W_{t+1} = W_t - \triangle \theta_t \tag{19}$$

$$\triangle \theta_t = \frac{\sqrt{v_t} + \epsilon}{\sqrt{h_t} + \epsilon} \frac{\partial E}{\partial W_t} \tag{20}$$

$$h_t = \rho h_{t-1} + (1-\rho) \left(\frac{\partial E}{\partial W_t} \right)^2 \tag{21}$$

$$v_t = \rho v_{t-1} + (1-\rho) \triangle \theta_t^2 \tag{22}$$

(5) Adam (Adaptive moments)

Adam uses the exponential averaging of the square of the slope of the RMSprop technique as a gradient descent method that combines the Momentum and RMSprop techniques (Eqs. (23)–(25)).

$$W_{t+1} = W_t - \eta \frac{1}{\sqrt{\hat{h}_t + \epsilon}} \hat{m}_t \tag{23}$$

$$\hat{m}_t = \frac{m_t}{1 - \beta_1^t} , \quad m_t = \beta_1 m_{t-1} + (1-\beta_1) \frac{\partial E}{\partial W_t} \tag{24}$$

$$\hat{v}_t = \frac{v_t}{1 - \beta_2^t} , \quad v_t = \beta_2 v_{t-1} + (1-\beta_2)(\frac{\partial E}{\partial W_t})^2 \tag{25}$$

Here, m_t is the estimate for the first moment of the gradient, v_t is the estimate for the second moment, and β_1 and β_2 are the correction values that correct the deviation of the weights.

3. Methodology

3.1 Experimental Database

It is required to consider various valuables to determine the wave transmission characteristics behind the LCS structure. The optimal machine learning model was used to figure out the role of variables affecting the wave control of LCS using the machine learning analysis package. We used the results of previous hydraulic experiment with LCS for input data, including deep sea wave length (L_0), crest freeboard (R_C), incident wave height (H_0), crown width (B), water depth (h), structure height (h_c), wave period (T_0), similarity coefficient for breakwater ($\tan\alpha$) and Dn_{50} (Seelig, 1980; Daemrich and kahle, 1985; van der Meer, 1988; Daemen, 1991) (Table 1). Data was obtained from DELOS databased of submerged breakwater information.

- 81 data on rubble mound emerged/submerged breakwater [Seelig];
- 95 data on tetrapod submerged breakwater [Daemrich and Kahle];
- 31 data on rubble mound emerged/submerged breakwater [Van der Meer];
- 53 data on rubble mound emerged/submerged breakwater [Daemen]

When applying the results of the mathematical model experiment, applying a dimensionless factor helps to clarify the problem related to the scale effect. Therefore, we applied 7 dimensionless factors as input variables as shown in Table 2 in consideration of the above dimension factors.

$$K_T = f\left\{ \frac{R_C}{H_0}, \frac{B}{H_0}, \xi, \frac{B}{L_0}, \frac{R_C}{h}, \frac{Dn_{50}}{h_c}, \frac{h_c}{h} \right\} \tag{26}$$

where R_C/H_0 is the relative freeboard, B/H_0 is the relative crest width, ξ is the surf similarity parameter, B/L_0 is the ratio of the crest width to the wavelength, R_C/h is the ratio of the crest height to the water depth, Dn_{50}/h_c is the ratio of the nominal diameter to the crest height, and h_c/h is the relative crest height. To reflect the same degree of feature scale, we converted the input variable using max-min normalization.

$$x_n = \frac{x - \min(x)}{\max(x) - \min(x)} \tag{27}$$

3.2 Hyperparameters Tuning and Model Validation

A machine learning model has many hyperparameters that the user

Table 1 Ranges of parameter of reference

	R_C		B		h		Dn_{50}		$\tan\alpha$		H_0		T_0	
	Min	Max	Min	Max	Min	Max	Min	Max	Min	Max	Min	Max	Min	Max
Seelig (1980)	−0.42	0.21	0.30	0.40	0.45	0.85	0.11	0.16	0.38	0.67	0.02	0.18	0.91	3.66
Damrich and Kahle (1985)	−0.20	0	0.20	1.00	0.50	0.70	0.08	0.08	0.50	0.50	0.02	0.23	1.23	3.27
Van der Meer (1988)	−0.10	0.13	0.3	0.3	0.4	0.4	0.03	0.03	0.5	0.5	0.08	0.23	1.94	2.60
Daemen (1991)	−0.09	0.20	0.34	0.34	0.27	0.52	0.04	0.06	0.67	0.67	0.03	0.15	0.98	2.88

Table 2 Definitions and ranges of scaled model parameter

Parameter		Definition	Average	Max	Min
X_1	R_C/H_0	Relative freeboard	-0.494	4.00	-8.696
X_2	B/H_0	Relative crest width	4.525	43.478	0.889
X_3	ξ	Surf similarity parameter	4.145	10.541	1.181
X_4	B/L_0	Ratio of the crest width to wave length	0.09	0.424	0.012
X_5	R_C/h	Ratio of the crest height to the water depth	-0.065	0.36	-0.56
X_6	Dn_{50}/h_c	Ratio of the nominal diameter to crest height	0.166	0.336	0.065
X_7	h_c/h	Relative crest height	0.935	1.734	0.44
Y	K_T	Transmission coefficient	0.482	0.922	0.049

Table 3 Hyperparameter tuning

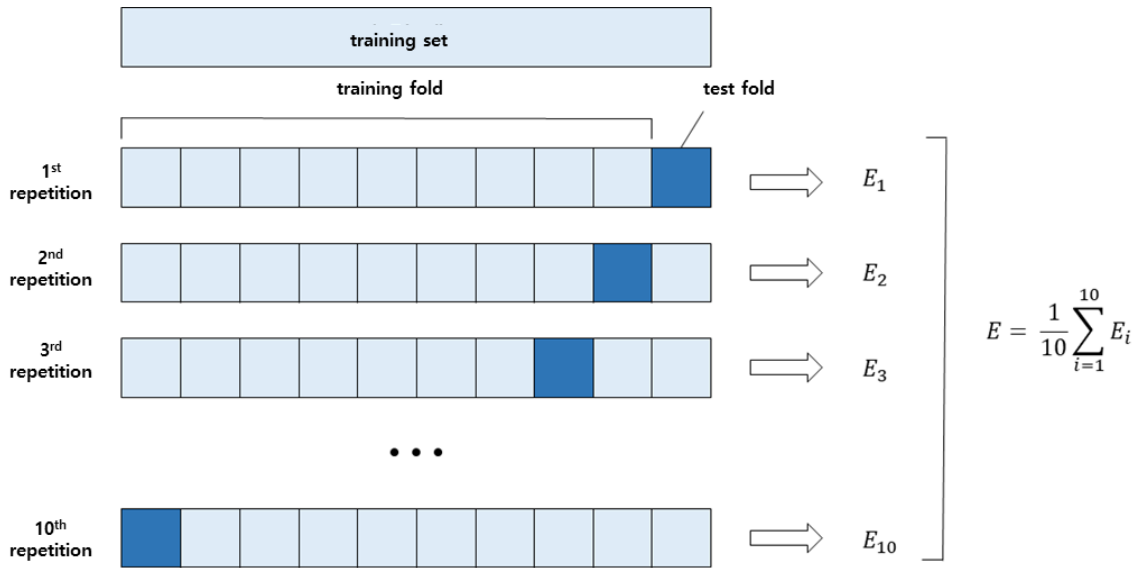| Hyper parameter	Range of hyperparameter	Number of hyperparameter
Hidden layer	1−2	2
Activation function of hidden layer	ReLU, Sigmoid, Tanh, Exponential	4
Hidden neuron	7−35 (15)	15
Output layer	1	1
Activation function of output layer	Sigmoid, Linear	2
Optimizer	SGD, Adadelta, Adagrad, Adam	4

Fig. 3 10-fold cross validation

needs to specify. It is used to optimize performance by balancing bias and variance of machine learning models. Random search cross-validation (CV) and grid search CV are methods for deriving hyperparameters suitable for models and data. In this study, the optimal parameters for predicting the wave height attenuation characteristics of low-rise structures were derived using grid search CV. Table 3 shows the parameters and ranges applied to the grid search CV, and the parameter with the highest accuracy was derived through the calculation of a total of 960 cases.

The purpose of a machine learning model is to predict with high accuracy on new data, and to ensure generalization and reliability of model performance on new data. Cross-validation is a method to improve the generalization performance of a model and is generally a more reliable and superior statistical evaluation method than dividing the training set and test set once. The most widely used cross-validation method is k-cross-validation, which was developed to minimize the bias associated with random sampling of the training set. In this study, 10-fold cross validation was performed, the entire data sample was divided into 10, 9 were used for training and 1 was used for model validation, and cross-validation was performed 10 times in a row (Fig. 3).

3.3 ANN Model Setup

Table 4 shows ANN model setup. In this study, we utilized the 260 sets of wave input data with reference to the results of the hydraulic model experiment with existing low crest structures. Of the total 260 data, we used 70% as training data and 30% as prediction data. To set up the prediction model of wave properties with high accuracy using LCS method, various hyperparameters were determined under different conditions, including the activation function, gradient descent technique, hidden layer, and overfitting prevention technique, to build a model with low error and high accuracy. With respect to the activation functions of the hidden layer and the output layer, optimal

activation functions (ReLU, Sigmoid) were applied using various model prediction results. We applied the calculated value to the hidden layer's activation function (ReLU) to explain non-linearity. We calculated the result by substituting the hidden layer calculation result into the function of output layers and output the result value by inputting it into the activation function (Sigmoid) of the output layer. To verify the model performance, we applied 10-fold cross-validation method that was developed to minimize the bias associated with random sampling of the training set.

The neural network derives an optimal weight and bias where the mean squared error (MSE) is minimized through the error backpropagation method. In the process of weight redistribution using backpropagation algorithm, the increase in the number of hidden layers and hidden nodes improves the model's performance, but increases training costs. Thus, this study determined various

Table 4 Model setup of ANN model

Total data	260
Training set	182
Test set	78
Normalization	Max-Min normalization
Input neuron	7
Hidden layer (Activation function)	1-2 (ReLU)
Hidden neuron	7-35
Output layer (Activation function)	1 (Sigmoid)
Epoch	10,000
Batch_size	200
Optimizer	Adam
Loss	Mean squared error
Overfitting prevention	Early stopping callback

hyperparameters with respect to the number of hidden layers and hidden neurons. We analyzed model accuracy (R^2) under the condition of the 1st–3th layers and 7–35 hidden neurons at hyperparameters.

When building a neural network, the optimal training time and prediction performance are obtained by varying the number of hidden layers and neurons. Fig. 4 reveals the R^2 results for the training set and the test set for the hidden neuron under the condition of different hidden layers, which shows trend lines with R^2 values with respect to the number of hidden layers and hidden neurons for training data. It represents that the model accuracy increases with the increase in the numbers of hidden layers. In addition, R^2 value of the training set gradually increases as the number of hidden neurons increases. On the other hand, the model accuracy of the test set increases as the number of hidden layers increases under certain condition (Fig. 5). The R^2 value (0.979) of the test set showed the highest accuracy under the condition of 29 hidden neurons with 2 hidden layers, which suggests that the model accuracy of the test set does have a high relationship with the accuracy of training set under certain condition. Thus, we constructed the model under the optimum condition of 29 hidden neurons with 2 hidden layers.
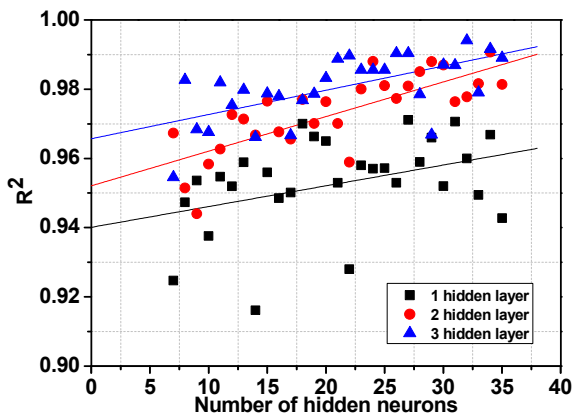

Fig. 4 R_squared of training data as a function of the number of hidden layer
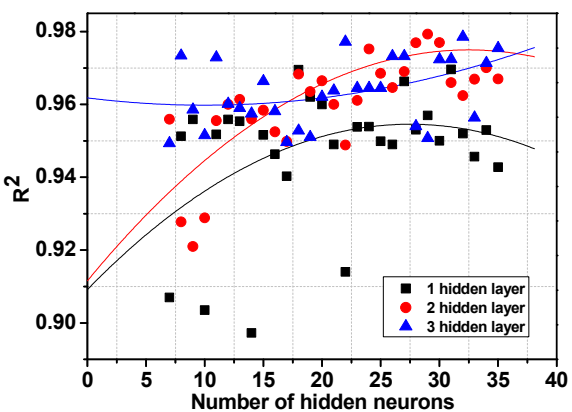

Fig. 5 R_squared of test data as a function of the number of hidden layer

4. Results and Discussion

4.1 Estimation of Wave Transmission Rate Using Empirical Formula

As shown in Fig. 6, we compared the experimental values of wave transmission rate with those obtained from empirical formula. Takayama et al. (1985) suggested an estimated wave transmission rate that has an MSE of 0.021 and an R^2 value of 0.5, which reveals the overestimation of experimental results with a low accuracy (Fig. 6(a)). Some data even broke the pattern of effective wave transmission rate ($0 < K_t < 1$), driven by the case of high relative freeboard. Takayama's formula can mainly use for the submerged structure under still water level, and the empirical formula are composed of the linear regression type of the 1st order of polynomial equation, which cause the low accuracy.

Among four different empirical formulas, Goda and Ahrens (2008) revealed the estimated wave transmission rate that has an MSE of 0.008 and an R^2 value of 0.851, which shows the highest accuracy because suggested formula used 6 types of dimensionless numbers for converted effective crest width (B_{eff}) under various conditions (Fig. 6(b)). Fig. 6(c) shows the estimated wave transmission rate of LCS suggested by Van der Meer et al. (2005). The effective values of wave transmission rate are obtained in the range of $0.075 < K_t < 0.8$ in the empirical formula. They provided an MSE of 0.009 and an R^2 value of 0.81, which generally represent overestimated results compared to experimental results. In the same manner, the results, obtained from Carabrese et al. (2003) provides the overestimated prediction at the point of wave transmission rate compared to the experimental results, as shown in Fig. 6(d), suggesting inappropriate model for our study.

4.2 Prediction Accuracy Analysis Using ANN

Figs. 7 and 8 show the wave transmission rate of the training and test data of 206 sets using a deep neural network under the optimum condition of 29 hidden neurons with 2 hidden layers. In the figures, the horizontal axis reveals the experimental values, and the vertical axis shows the distribution of predicted values. In the prediction results of the training dataset, index of agreement (I) was 0.997, scatter index (SI) was 0.086, and R^2 was 0.988. For the test dataset, MSE was 1.3×10^{-3}, I was 0.995, SI was 0.078, and R^2 was 0.979, suggesting that the predictive model for the wave transmission rate demonstrated excellent performance. Based on the obtained analysis, it is worth noting that the performance prediction method using an artificial neural network model can be suitable for various fields in coastal engineering, unlike the broadly used empirical formula. Table 5 shows the statistical model performance results based on the application of popular empirical formula compared to deep neural network, which suggests that the ANN model provides a more accurate prediction performance compared to the empirical formula. In addition, the ANN model is not required to set up the effective range of the wave transmission rate or apply the special formula dependent on the input variables whereas the empirical formula can be used under the recommended effective range in order to diminish the uncertainty.
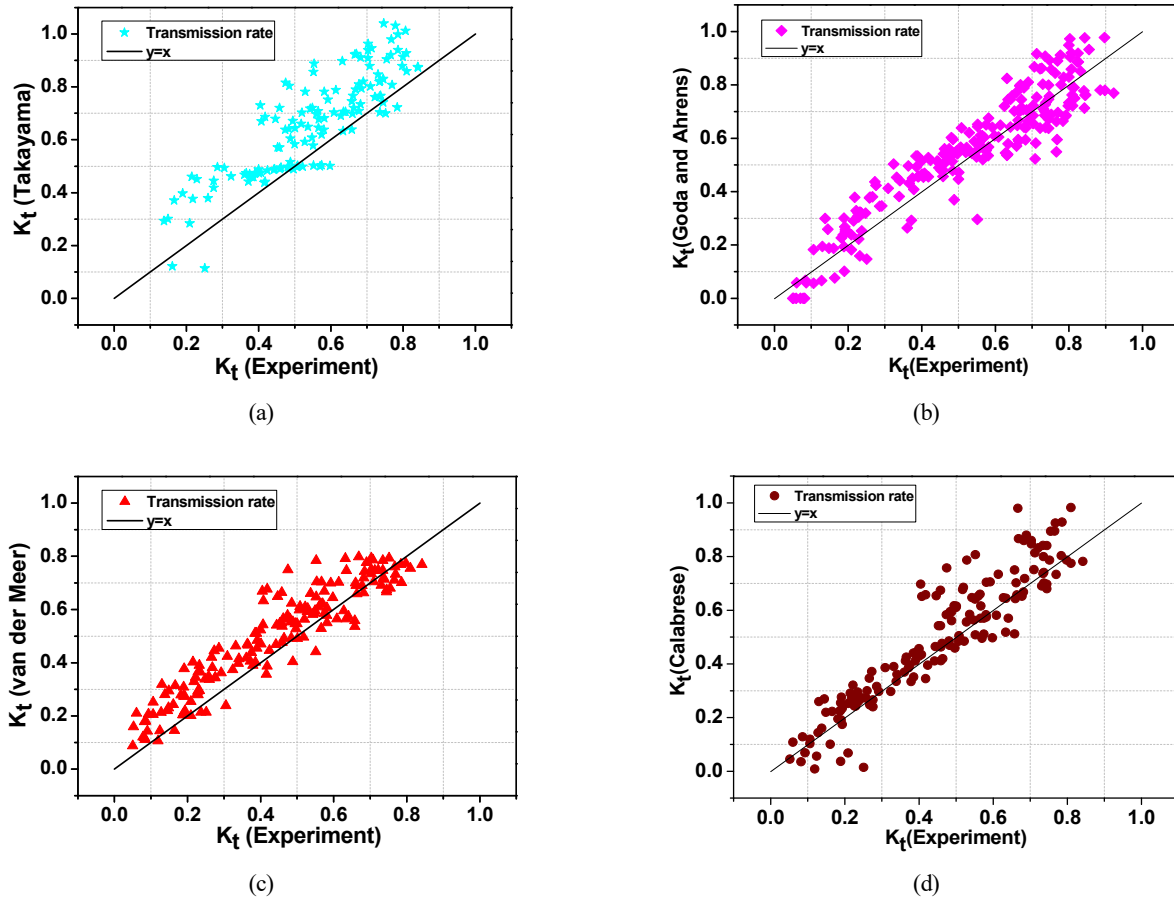
(a)

(b)

(c)

(d)

Fig. 6 Comparison of wave transmission formulas with experimental data: (a) Takayama et al. (1985); (b) Goda and Arhens. (2008); (c) Van der Meer et al. (2005); (d) Calabrese et al. (2003)

Table 5 Statistical parameters of the results

Methods	MSE	I	SI	R^2
Takayama et al. (1985)	21×10^{-3}	0.846	0.263	0.500
Goda and Arhens (2008)	8×10^{-3}	0.962	0.172	0.851
Van der Meer (2005)	9×10^{-3}	0.974	0.221	0.810
Calabrese et al. (2003)	9×10^{-3}	0.952	0.215	0.792
ANN model	1.3×10^{-3}	0.995	0.078	0.979

Note: MSE = Mean square error, I = Index of agreement, SI = Scatter index

Thus, the ANN model can provide high prediction accuracy with cost-effective reliability when only seven dimensionless input variables are used.

4.3 Sensitivity Analysis

To estimate the independent importance of the input variable of the model constructed using ANN calculations and to determine the important input variables, we performed a sensitivity analysis of the effect on the prediction of the wave transmission rate through model application using the same training set. Table 6 shows the sensitivity analysis results of the wave transmission rate for each input variable. To estimate the independent importance of the input variable of the model constructed using ANN calculations and to determine the

important input variables, we performed sensitivity analysis of the effect on the prediction of the wave transmission rate through model application using the same training set. The analysis reveals that the model accuracy for the relative freeboard (R_C/H_0) had an MSE of 146.7×10^{-3} and an R^2 value of 0.153, which was found to be the most important parameter for the wave attenuation and wave transmission rate of the structure. This finding is attributed to the reduction of transmitted wave height along with strong breaking wave, and an increased reflected wave in front of the structure as the crown depth is reduced. Figs. 9 (a) and (d) are the distributions of the experimental and predicted values, respectively, when factors related to the relative freeboard and ratio of the crest height to the water depth are excluded, which showed that the predicted value using the model overestimated
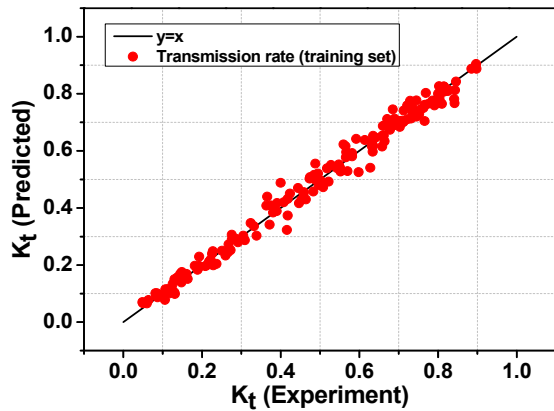
Fig. 7 Comparison of transmission rate between experiment and prediction (training data)
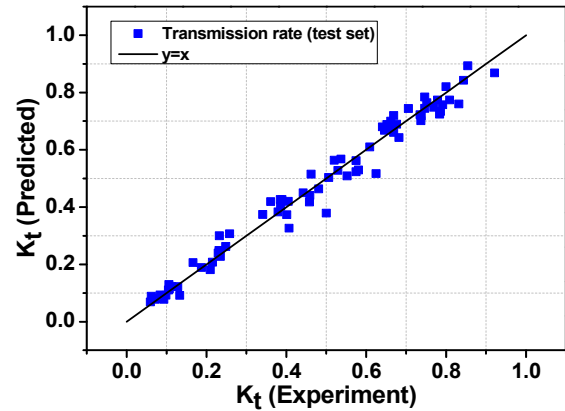

Fig. 8 Comparison of transmission rate between experiment and prediction (test data)

the experimental value and the error increased significantly. As the relative freeboard factor is the dominant factor in wave control, a large error occurred when the two factors were not considered.

Most of empirical formular(van der Meer, 2005; Goda, 2008; Calabrese, 2003; Takayama, 1985) have suggested r elative freeboard (R_C/H_0), ratio of the crest width to wave length (B/L_0) and surf similarity parameter (ξ) as impact factors for wave attenuation coefficient. However, sensitivity to the wave breaking similarity coefficient reflecting the conditions for the front slope and wave slope

of the structure was MSE 22.4×10^{-3}, R^2 0.703, which was less sensitive to wave control than other variables. The standard deviation of the input variable is large, and the interpretation of various conditions of the crest width to wave length is insufficient because wave transmission rate was performed for two widths of 0.3 and 1.0, in the input variable. In all experiments and model implementation, the variable control is considered one of the important factors for obtaining reliable results. Therefore, in future research, we plan to develop a model with high predictive performance through the

Table 6 Sensitivity analysis of ANN model

Parameter		Performance measures			
		MSE	I	SI	R^2
X_1	R_C/H_0	146.7×10^{-3}	0.589	0.795	0.153
X_2	B/L_0	9.7×10^{-3}	0.962	0.205	0.864
X_3	ξ	22.4×10^{-3}	0.925	0.311	0.703
X_4	B/L_0	27.0×10^{-3}	0.896	0.341	0.684
X_5	R_C/H	78.3×10^{-3}	0.665	0.581	0.343
X_6	Dn_{50}/h_c	40.1×10^{-3}	0.832	0.416	0.563
X_7	h_c/h	45.4×10^{-3}	0.818	0.443	0.572
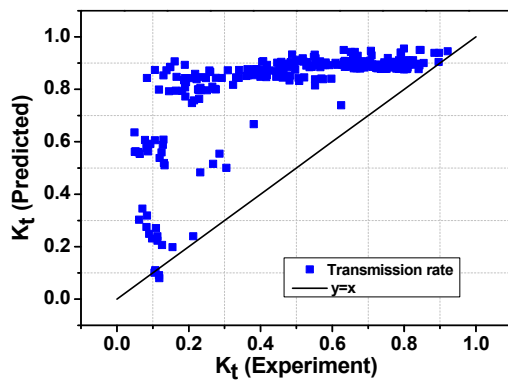
(a)
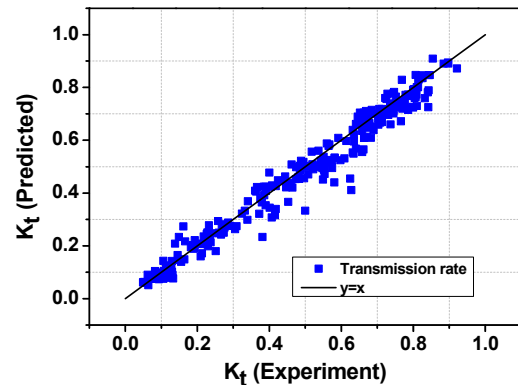
(b)

Fig. 9 Sensitivity analysis of input variables: (a) R_C/H_0 variables of sensitivity; (b) B/H_0 variables of sensitivity; (c) ξ variables of sensitivity; (d) B/L_0 variables of sensitivity; (e) R_C/h variables of sensitivity; (f) Dn_{50}/h_c variables of sensitivity; (g) h_c/h variables of sensitivity

(c)

(d)

(e)

(f)

(g)

Fig. 9 Sensitivity analysis of input variables: (a) R_C/H_0 variables of sensitivity; (b) B/H_0 variables of sensitivity; (c) ξ variables of sensitivity; (d) B/L_0 variables of sensitivity; (e) R_C/h variables of sensitivity; (f) Dn_{50}/h_c variables of sensitivity; (g) h_c/h variables of sensitivity (Continuation)
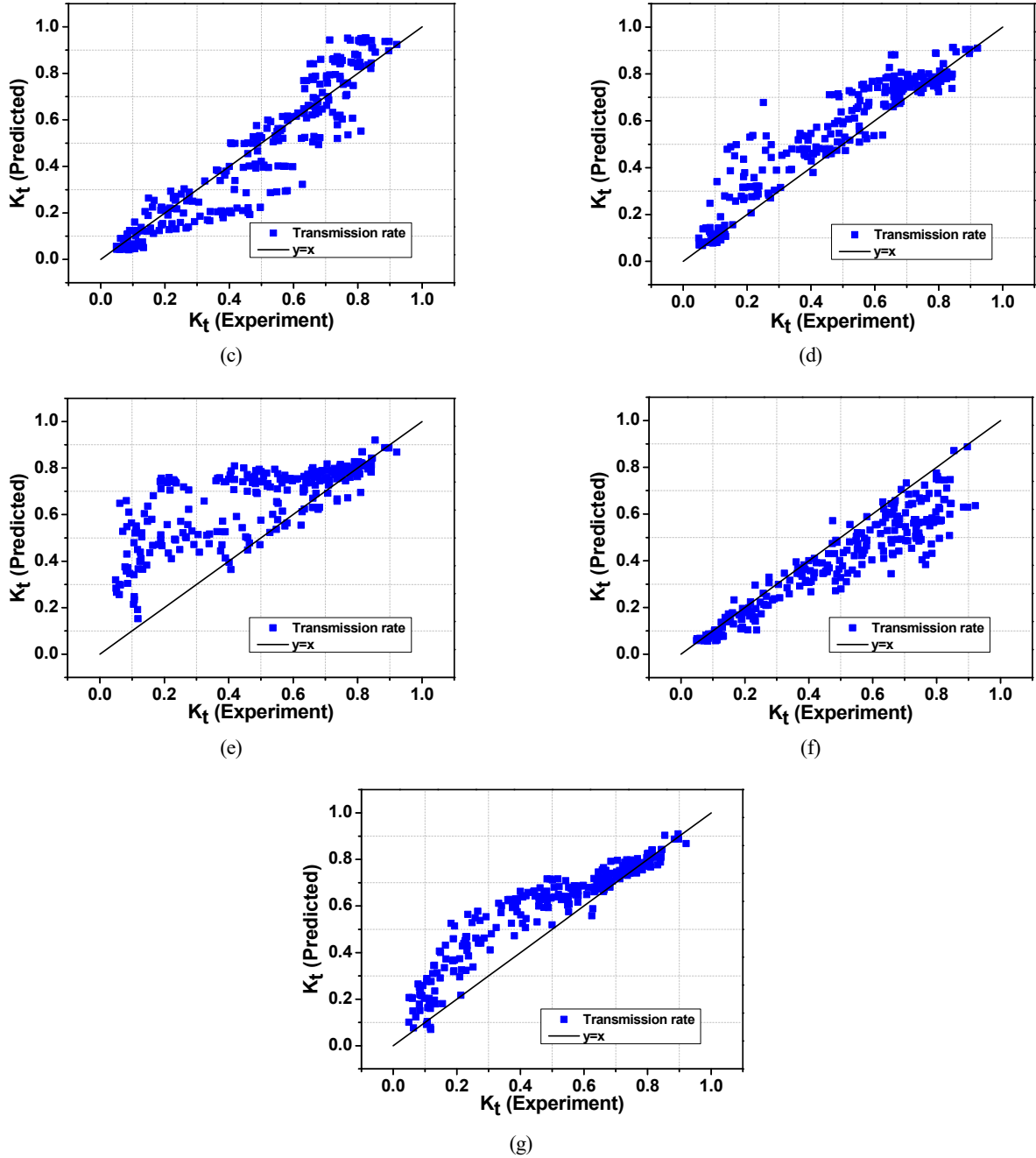
development of various machine learning-based predictive models using refined input variables.

4.4 Analysis of Accuracy Metric According to Input Variables Combination

In this study, we applied input variables composed of seven dimensionless numbers ($X = \{X_1 : \frac{R_C}{H_0}$, $X_2 : \frac{B}{H_0}$, $X_3 : \xi$, $X_4 : \frac{B}{L_0}$, $X_5 : \frac{R_C}{h}$, $X_6 : \frac{Dn_{50}}{h_c}$, $X_7 : \frac{h_c}{h}\}$) and analyzed the effect on model

performance when some input variables or data were not reflected through various combinations. The results of the predicted values and the experimental values using eight combinations are shown in Fig. 10, and model performance results according to the eight combinations of input variables are shown in Table 7. Combination 1 shows the model performance results when the seven non-dimensional input variables are applied, indicating highest accuracy with an MSE of 1.3×10^{-3} and R^2 of 0.979.

Combination 7, applying three input variables ($X_2 : \frac{B}{H_0}, X_3 : \xi$,

$X_4 : \dfrac{B}{L_0}$, $X_6 : \dfrac{Dn_{50}}{h_c}$), showed the lowest accuracy with an MSE of 38.7×10^{-3} and R^2 of 0.401. In addition, combination 8 with same variables applied ($X_1 : \dfrac{R_C}{H_0}$, $X_5 : \dfrac{R_C}{h}$, $X_7 : \dfrac{h_c}{h}$) showed relatively good accuracy, with an MSE of 6.7×10^{-3}, and R^2 of 0.896. The analysis results from various combinations suggest that the accuracy does not increase linearly even if the number of input variables increases.

Furthermore, accurate prediction using neural network model requires reducing training time and improving the simplicity of the model. An ideal model is one that describes the problem in the easiest and simplest way using the fewest variables. Therefore, it is important to identify variables that save modeling time and space.

Accordingly, combination 4 using four input variables produced a result with relatively high accuracy, with an MSE of 2.5×10^{-3} and R^2 of 0.961. In terms of the model time cost, combination 4 offers a good alternative for the model.

Table 7 Performance measures for analysis of different input variable combinations

| Combinations	MSE	Performance measures					
		I		SI		R2	
		test	train	test	train	test	train
1: $X_1, X_2, X_3, X_4, X_5, X_6, X_7$	1.3×10^{-3}	0.995	0.997	0.078	0.086	0.979	0.988
2: $X_2, X_3, X_4, X_5, X_6, X_7$	1.9×10^{-3}	0.992	0.994	0.095	0.080	0.970	0.975
3: X_1, X_4, X_5, X_6, X_7	2.7×10^{-3}	0.989	0.99	0.112	0.100	0.958	0.961
4. X_1, X_2, X_3, X_4, X_6	2.2×10^{-3}	0.991	0.994	0.100	0.077	0.966	0.977
5. X_1, X_4, X_5, X_7	2.5×10^{-3}	0.990	0.994	0.107	0.076	0.961	0.977
6. X_2, X_3, X_4, X_6	37.4×10^{-3}	0.807	0.919	0.414	0.265	0.424	0.632
7. X_2, X_3, X_6	38.7×10^{-3}	0.791	0.902	0.422	0.285	0.401	0.552
8. X_1, X_5, X_7	6.7×10^{-3}	0.973	0.977	0.175	0.150	0.896	0.906
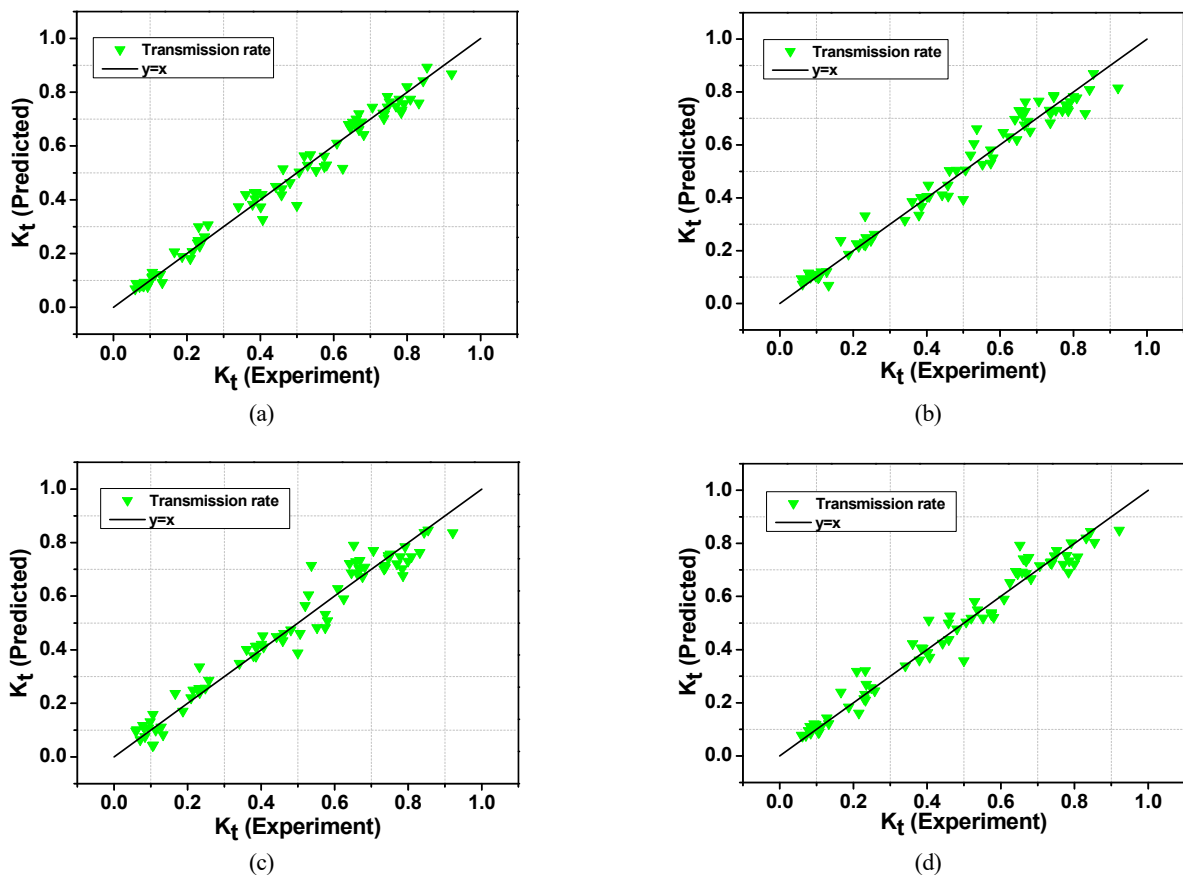
(a)

(b)

(c)

(d)

Fig. 10 Influence of number of input; variables: (a) Combination 1; (b) Combination 2; (c) Combination 3; (d) Combination 4; (f) Combination 6; (g) Combination 7; (h) Combination 8

Fig. 10 Influence of number of input; variables: (a) Combination 1; (b) Combination 2; (c) Combination 3; (d) Combination 4; (f) Combination 6; (g) Combination 7; (h) Combination 8 (Continuation)
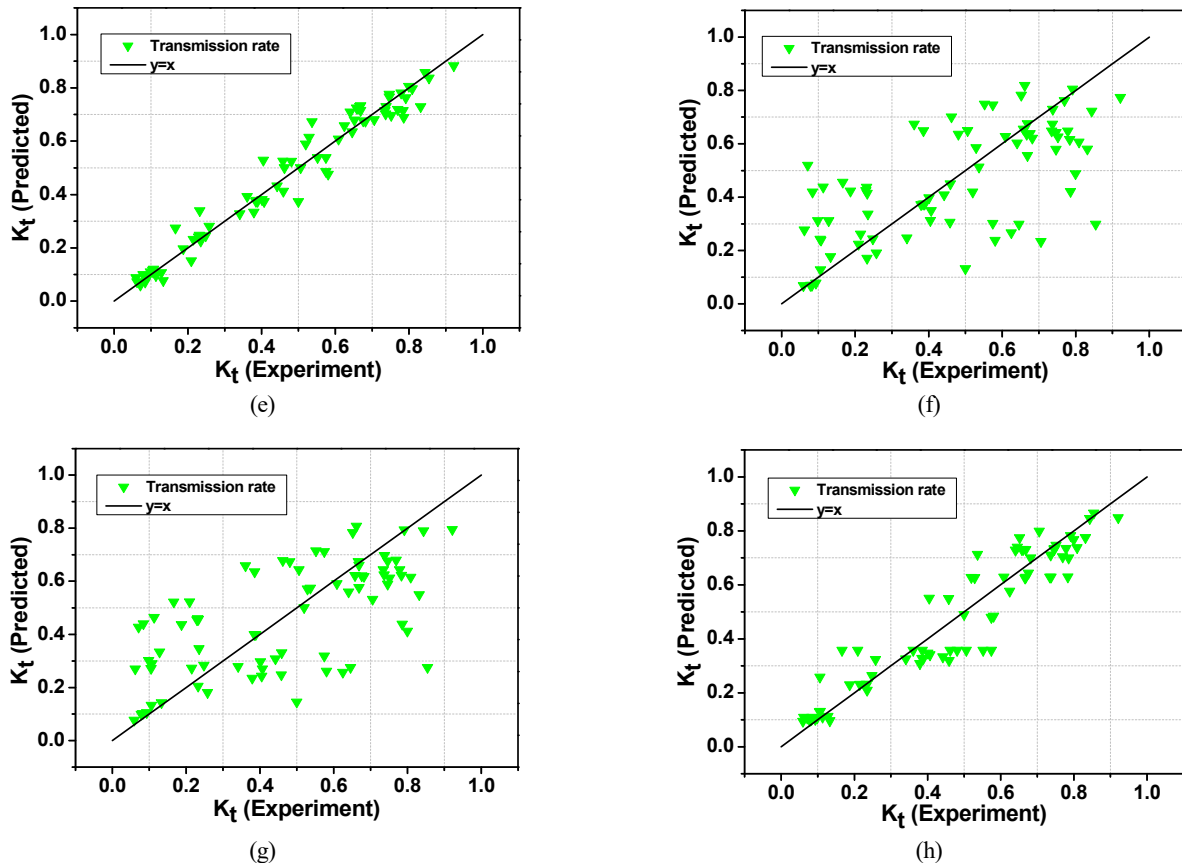
4. Conclusion

In this study, we built a deep neural network model to predict the wave transmission rate of low crested structures using TensorFLow, an open source platform. To construct the model, we utilized the hydraulic model experiment data from Seelig (1980), Daemrich and kahle (1985), van der Meer (1988), Daemen (1991) for training (70%) and prediction (30%). These neural network models show reliable prediction performance and are expected to be widely used in practical applications in the field of coastal engineering.

The sensitivity analysis using the neural network model found that importance of independent variable input for relative freeboard (R_C/H_0) and ratio of the crest height to the water depth (R_C/h) was large, and the lowest performance appeared when the two factors were excluded from training. In short, the crest depth was found to be the most dominant factor influencing the wave height attenuation in the hydraulic behavior around the low crested structure.

The proposed model showed relatively high accuracy in predicting the wave transmission coefficient of the low crested structure according to various combinations of input variables, with combination 5 showing 0.961 despite using a small number of input variables. In terms of the model time cost, a method using combination 5 offers a good alternative.

The prediction results were analyzed using a comparative review of

the results from the existing empirical formula and statistical indicators. The result of wave transmission rate of the trained deep neural network model showed very good prediction accuracy, with 1.3×10^{-3} of MSE, 0.995 of I, 0.078 of SI, and 0.979 of R^2, the prediction performance is highly improved compared to existing empirical results. Engineers and scientists can use the suggested model as a design tool to predict the wave transmission coefficient behind the low crested structure.

Conflict of Interest

Soonchul Kwon serve as an editor of the Journal of Ocean Engineering and Technology but has no role in the decision to publish this article. No potential conflict of interest relevant to this article was reported.

Funding

References

Calabrese, M., Vicinanza, D., & Buccino, M. (2003). 2D wave set up

behind low crested and submerged breakwaters. *Proceedings of the 13th International Conference ISOPE, Honolulu, Hawaii, USA.* https://onepetro.org/ISOPEIOPEC/proceedings/ISOPE03/All-ISOPE03/ISOPE-I-03-321/8542

Daemen, I. F. R. (1991). *Wave transmission at low-crested structures* [Master thesis, Delft University of Technology]. Delft Hydraulics Report H462.http://resolver.tudelft.nl/uuid:433dfcf3-eb87-4dc9-88dc-8969996a6e3f

Daemrich, K., & Kahle, W. (1985). Protective effect of underwater breakwaters under the influence of irregular sea waves (Report Heft 61). Franzius-Instituts fur Wasserbau und Kusteningenieurswesen.

Formentin, S. M., Zanuttigh, B., & Van der Meer, J. W. (2017). A Neural network tool for predicting wave reflection, overtopping and transmission. *Coastal Engineering Journal, 59(1)*, 1750006. https://doi.org/10.1142/S0578563417500061

Goda, Y., & Ahrens, J. P., (2008). New formulation of wave transmission over and through low-crested structures. *Proceedings of the 31st International Conference of Coastal Engineering, Hamburg, Germany,* 3530−3541. https://doi.org/10.1142/9789814277426_0292

Hashemi, M. R., Ghadampour, Z., & Neill, S. P. (2010). Using an artificial neural network to model seasonal changes in beach profiles. *Ocean Engineering, 37*(14-15), 1345−1356. https://doi.org/10.1016/j.oceaneng.2010.07.004

Kim, D. H., & Park, W. S. (2005). Neural network for design and reliability analysis of rubble mound breakwaters. *Ocean engineering, 32*(11-12), 1332−1349. https://doi.org/10.1016/j.oceaneng.2004.11.008

Koosheh, A., Etemad-Shahid, A., Cartwright, N., Tomlinson, R., & Hosseinzadeh, S. (2020). The comparison of empirical formulae for the prediction of mean wave overtopping rate at aromored sloped structures. *Coastal Structure, 36v.* https://icce-ojs-tamu.tdl.org/icce/index.php/icce/article/view/10161

Lee, J. H., Jung, W. J., Bae, J. H., Lee, K. H., & Kim, D. S. (2019). Variation characteristic of wave field around 2-dimensional low-crested-breakwaters. *Journal of Korean Society of Coastal and Ocean Engineers, 31*(5), 294−304. https://doi.org/10.9765/KSCOE.2019.31.5.294

Lee, J. I., & Bae, I. L. (2020). Experimental study for wave transmission coefficients of submerged structure : Ⅰ. Permeable type structure. *Journal of the Korean Society of Civil Engineers, 40*(5), 485−496. https://doi.org/10.12652/Ksce.2020.40.5.0485

Panizzo, A., & Briganti, R. (2007). Analysis of wave transmission behind low-crested breakwaters using neural networks. *Coastal Engineering, 54*(9), 643−656. https://doi.org/10.1016/j.coastaleng.2007.01.001

Rigos, A., Tsekouras, G. E., Chatzipavlis, A., & Velegrakis, A. F. (2016). Modeling beach rotation using a novel legendre polynomial feedforward neural network trained by nonlinear constrained optimization. In *IFIP International Conference on Artificial Intelligence Applications and Innovations* (pp. 167−179). Springer International Publishing.

Seelig, W. N. (1980). *Two dimensional tests of wave transmission and feflection characteristics of laboratory breakwaters* (Technical report No. 80-1). Coastal Engineering Research Center, U.S. Army, Corps of Engineers Waterways Experiment Station, Vicksburg, MS, 187. https://apps.dtic.mil/sti/pdfs/ADA089603.pdf

Shamshirband, S., Mosavi, A., Rabczuk, T., Nabipour, N., & Chau, K. W. (2020). Prediction of significant wave height; comparison between nested grid numerical model, and machine learning models of artificial neural networks, extreme learning and support vector machines. *Engineering Applications of Computational Fluid Mechanics, 14*(1), 805−817. https://doi.org/10.1080/19942060.2020.1773932

Takayama, T., Nagai, K., & Sekiguchi, T. (1985). Irregular wave experiments on wave dissipation function of submerged breakwater with wide crown. In *Proceedings of 32th Japanese Conference on Coastal Engineering, JSCE,* (Vol. 32, pp. 545−549)

Van der Meer, J. W. (1988). *Rock slopes and gravel beaches under wave attack* [PhD thesis, Delft University of Technology]. Delft Hydraulics Report 396.

Van der Meer, J. W., Briganti, R., Zanuttigh, B., & Wang, B. (2005). Wave transmission and reflection at low-crested structures: Design formulae, oblique wave attack and spectral change. *Coastal Engineering, 52*(10−11), 915−929. https://doi.org/10.1016/j.coastaleng.2005.09.005

Author ORCIDs

Author name	ORCID
Kim, Taeyoon	0000-0002-5060-5302
Lee, Woo-Dong	0000-0001-7776-4664
Kwon, Yongju	0000-0001-7935-8416
Kim, Jongyeong	0000-0001-6642-8622
Kang, Byeonggug	0000-0003-4057-4386
Kwon, Soonchul	0000-0003-3764-331X